The Journal of Physiology

J Physiol 592.24 (2014) pp 5477–5492

The determinants of transverse tubular volume in resting skeletal muscle

Jingwei Sim and James A. Fraser

Physiological Laboratory, University of Cambridge, Downing Street, Cambridge CB2 3EG, UK

Key points

- The surface membrane of skeletal muscle infolds to form a system of transverse (t)-tubules, which propagate electrical activity deep into the fibre to activate muscle contraction.
- Ionic currents flowing into and out of the t-tubules can cause osmotic fluxes and tubular volume changes, such as those seen in muscle fatigue and trauma, but the mechanisms driving these are unclear.
- We used a computer model to determine that resting t-tubule volume is maintained by active ion cycling between the extracellular fluid, muscle cell and t-tubules.
- By considering how these ion cycles are influenced by the extracellular fluid composition, we can reliably predict the resultant changes in t-tubule volume.
- These findings explain and reconcile previous experimental data, providing a framework for understanding the role of the t-system in muscle physiology and pathology.

Abstract The transverse tubular (t)-system of skeletal muscle couples sarcolemmal electrical excitation with contraction deep within the fibre. Exercise, pathology and the composition of the extracellular fluid (ECF) can alter t-system volume (t-volume). T-volume changes are thought to contribute to fatigue, rhabdomyolysis and disruption of excitation–contraction coupling. However, mechanisms that underlie t-volume changes are poorly understood. A multicompartment, history-independent computer model of rat skeletal muscle was developed to define the minimum conditions for t-volume stability. It was found that the t-system tends to swell due to net ionic fluxes from the ECF across the access resistance. However, a stable t-volume is possible when this is offset by a net efflux from the t-system to the cell and thence to the ECF, forming a net ion cycle ECF→t-system→sarcoplasm→ECF that ultimately depends on Na^+/K^+-ATPase activity. Membrane properties that maximize this circuit flux decrease t-volume, including $P_{Na(t)} > P_{Na(s)}$, $P_{K(t)} < P_{K(s)}$ and $N_{(t)} < N_{(s)}$ [P, permeability; N, Na^+/K^+-ATPase density; (t), t-system membrane; (s), sarcolemma]. Hydrostatic pressures, fixed charges and/or osmoles in the t-system can influence the magnitude of t-volume changes that result from alterations in this circuit flux. Using a parameter set derived from literature values where possible, this novel theory of t-volume was tested against data from previous experiments where t-volume was measured during manipulations of ECF composition. Predicted t-volume changes correlated satisfactorily. The present work provides a robust, unifying theoretical framework for understanding the determinants of t-volume.

(Received 21 July 2014; accepted after revision 13 October 2014; first published online 4 November 2014)
Corresponding author J. A. Fraser: Physiological Laboratory, University of Cambridge, Downing Street, Cambridge CB2 3EG, UK. Email: jaf21@cam.ac.uk

Abbreviations E, membrane potential; ECF, extracellular fluid; N, Na^+/K^+-ATPase density; P_{ion}, background ion leak permeability; R_A, tubular access resistance; subscript e, extracellular compartment; subscript i, intracellular compartment; subscript $t(n)$, transverse tubule nth shell from surface; t-system, transverse tubular system; t-volume, transverse tubular volume; V, volume; z_X, valency (mosmol^{-1}) and [X] concentration (mosmol l^{-1}) of fixed solutes.

DOI: 10.1113/jphysiol.2014.281170

Introduction

The transverse tubular (t)-system of skeletal muscle couples electrical excitation at the surface membrane with contraction deep within the muscle fibre. Although the t-system lumen is continuous with the extracellular fluid (ECF), t-system volume (t-volume) is labile, ranging from <0.5% of fibre volume in resting muscle to as much as 10–15% in fibres undergoing vacuolation in response to glycerol withdrawal from amphibian and mammalian muscle (Krolenko & Lucy, 2001). Excursions in t-volume have also been seen in exercise, rhabdomyolysis, dystrophy (Atkinson *et al.* 1981), trauma (Casademont *et al.* 1988) and accompanying changes in extracellular ion concentrations (Foulks *et al.* 1965; Rapoport *et al.* 1969; Dulhunty, 1982) or osmolality (Franzini-Armstrong *et al.* 1978; Launikonis & Stephenson, 2002). As t-volume changes can disrupt excitation–contraction coupling and calcium release (Martin *et al.* 2003), they may also play a role in muscle fatigue.

Factors determining t-volume at rest and during activity or pathology remain unclear. There is probably no single determinant of t-volume. T-volume may change even when muscle fibre volume does not, as seen in isometric tetani (Lännergren *et al.* 2000) and isotonic Cl^- withdrawal (Dulhunty, 1982). Studies that suggest t-volume is greatly influenced by ECF osmolality, ionic strength or membrane potential have led to apparently conflicting results (Rapoport *et al.* 1969; Dulhunty, 1982; Launikonis & Stephenson, 2002). However, enough experimental evidence is available to parameterize and test a computational model of the skeletal muscle fibre that could explore the mechanisms of t-volume determination and regulation. A multicompartment computer model of rat skeletal muscle was thus developed after Fraser *et al.* (2011*a*) to define the minimum conditions for t-volume stability, as well as the mechanisms of t-volume changes under a wide range of conditions. The model was built on charge difference principles to ensure strict conservation of the relationships between ion concentrations, osmolality, membrane potentials and compartment volumes (Fraser & Huang, 2004, 2007). Simulations were then performed to determine the influence of key electrophysiological parameters – hydrostatic pressures, membrane-impermeant ions, ion permeabilities and Na^+/K^+-ATPase densities – on t-volume.

The model demonstrates that with physiologically reasonable parameter sets, there is a net ion influx from the ECF across the access resistance. To maintain a stable t-system, cellular osmotic contents and cellular volume, net ion fluxes from the ECF into the t-system must match those moving from the t-system into the sarcoplasm, and from the sarcoplasm to the ECF at steady state. This forms a net ECF → t-system → sarcoplasm → ECF ion cycle that ultimately depends on Na^+/K^+-ATPase activity. Conditions that reduce this circuit flux predictably cause t-volume swelling.

This novel theory of t-volume determination was tested by comparing the model's predictions with previously published experimental data on isolated mammalian or amphibian muscle fibre preparations. The model correctly predicted the direction of volume changes reported in all available studies, supporting the theory that t-volume changes in the presence of different extracellular solute compositions could be understood as changes to individual ion cycles, or in the properties of fixed charges in the t-system. This study therefore provides a robust, unifying framework for understanding the determinants of t-volume.

Methods

A multicompartment model of transverse tubular volume

An iterative, multicompartment computer model of a rat skeletal muscle fibre was used as previously described by Fraser *et al.* (2011). It is depicted in Fig. 1 simulating a muscle fibre and t-system communicating with an ECF compartment of infinite volume. The ECF and sarcoplasm are separated by the surface membrane. The t-system is subdivided into a number of multiple concentric shells separated by luminal resistances in series, with the most superficial t-system shell linked to the ECF by an access resistance, R_A, permissive to all ECF solutes. Most simulations were performed in a model with 20 t-system shells. Some simulations employed a model fibre with only five t-system shells to allow large parameter sets to be processed rapidly. Representative simulations for each parameter set were then repeated in a 20-shell model to ensure that simulation results were not influenced by the artificial subdivision of the t-system into shells. Each t-system shell is separated from the cell by the tubular membrane. The membrane permeabilities and Na^+/K^+-ATPase density of the sarcolemma and tubular membrane could be varied independently.

Transmembrane, electrodiffusive and Na^+/K^+-ATPase fluxes were modelled as described previously (Fraser *et al.* 2011). Intercompartment potentials were calculated from the difference between cation and anion charge concentrations in each compartment:

$$E_m = \frac{\left([Q]_i + \sum_{n=0}^{n=\max} [Q]_{t(n)} V_{t(n)}\right)}{(C_m A_m)} \quad (V)$$

$$E_{t(n)} = \frac{-[Q]_{t(n)} V_{t(n)}}{C_m A_{t(n)}} \quad (V)$$

Where E_m is the surface membrane potential (V), $E_{t(n)}$ the tubular membrane potential for each of n t-system shells (V), V is the volume of each compartment (l), C_m the unit membrane capacitance (F cm^{-2}), A the membrane area (cm^{-2} l^{-1}) and $[Q]$ the net charge, calculated as $[Q] = F([Na^+] + [K^+] - [Cl^-] + z_X[X])$ for each compartment. This charge difference approach allows relationships between charge, currents, concentrations and osmolality to be conserved strictly (Fraser & Huang, 2007).

Model parameterization

Values of total ion permeabilities, water permeability and capacitance appropriate for modelling the electrophysiology of rat skeletal muscle were chosen (Fraser *et al.* 2011). Capacitance and water permeability were assumed similar for the surface and t-system membranes per unit area, taken as 156 μm s^{-1} (Frigeri *et al.* 2004). The osmotic and hydrostatic forces that might result from the physical structure of the t-system and its contents were also simulated. Transmembrane water fluxes were calculated according to the osmotic gradient and the hydraulic permeability of the membrane. Water fluxes between t-system shells and across the access resistance depend on the osmotic gradient and the diffusivity of water in dilute solutions, taken as 2.3×10^{-7} dm^2 s^{-1} (Tanaka, 1978). In all cases, compartment volumes changed according to the net uptake or efflux of water.

To define the minimum conditions for t-volume stability with this model, we varied the distributions of ion permeabilities and Na^+/K^+-ATPase densities between the surface and tubular membranes in turn, while keeping the solute composition of the ECF constant. When determining the effect of ECF solutes on t-volume, a stable, 'baseline' t-system was used consistently; its parameter set was derived from literature values where possible (Table 1).

Constraints of hydrostatic pressure in the transverse tubular system

We addressed the consequences of various physical constraints on the t-system. As t-volume can change profoundly (Rapoport *et al.* 1969; Dulhunty, 1982), the

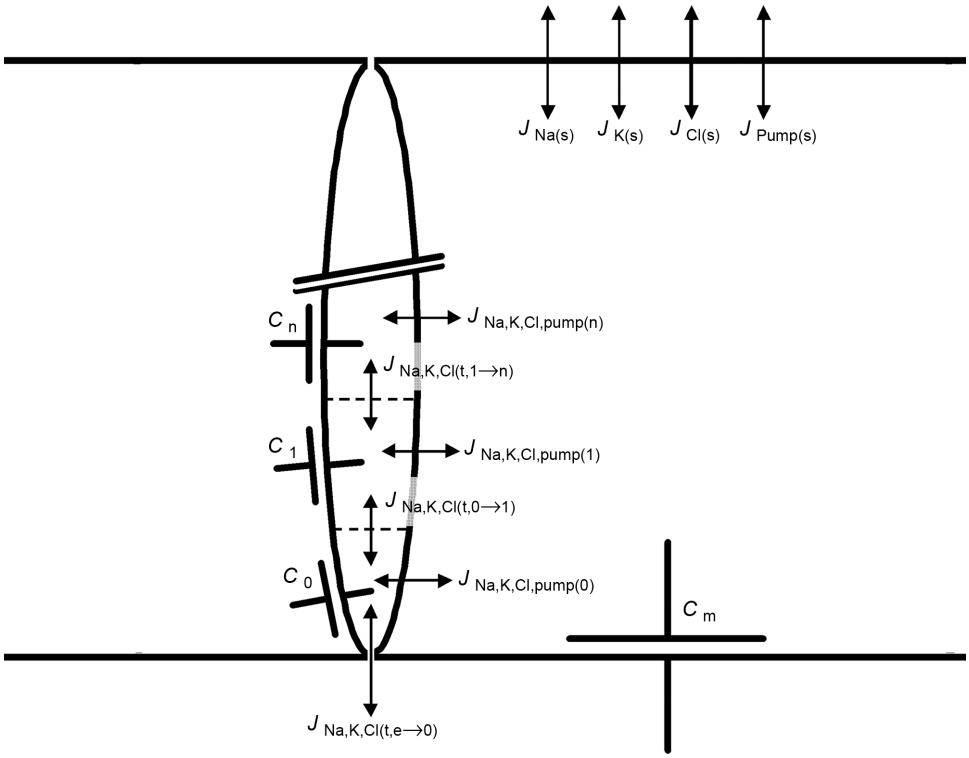

Figure 1. Schematic showing relationships between extracellular fluid (ECF), t-system and muscle cell, modelled as multiple compartments
Rat skeletal muscle fibre segment was modelled as an array of compartments – the ECF, sarcoplasm and t-system as a series of n uniformly thick concentric shells, each shell sharing in total t-system membrane capacitance (C) and ionic permeabilities according to its fractional volume. The potential of each compartment was calculated using charge-difference principles (Fraser *et al.* 2011). Ionic fluxes (J) across the sarcolemma, t-system membranes and t-system luminal resistances were also modelled. Water movements between each compartment were calculated as described in Methods. This model was used to investigate the minimum conditions for a stable t-system at rest.

Table 1. Base–case parameters of the model

Parameters			
Symbol	Description	Value	Reference
A_m	Surface membrane area	769231 cm^2 l^{-1}	Fraser *et al.* (2011)
A_t	T-system membrane area	3076924 cm^2 l^{-1}	
V_t	Relative t-system volume	0.0039 l l^{-1}	
C_m	Membrane capacitance	1×10^{-6} F cm^{-2}	
R_A	T-system access resistance	72.3 Ω cm^2	
g_t	T-system lumen inter-shell conductance	0.0037 S cm^{-1}	Wallinga *et al.* (1999)
σ_t	T-system tortuosity factor	0.21	
$[ATP]_i$	Intracellular ATP concentration	6 mM	Hernandez *et al.* (1989); Thompson & Fitts (1992)
$[ADP]_i$	Intracellular ADP concentration	0.006 mM	
$[P_i]_i$	Intracellular inorganic phosphate	4.95 mM	
z_{Xi}	Mean intracellular fixed charge valency	−1.6477	Maughan & Recchia (1985); Maughan & Godt (2001)
N_s	Surface membrane Na^+/K^+ pump density	9×10^{-12} cm^{-2}	Model derived, to maintain $[Na^+]_i$ in reasonable range
N_t	Tubular membrane Na^+/K^+ pump density	4.5×10^{-12} cm^{-2}	
$P_{Na(s)}$	Surface membrane background Na^+ permeability	2.16×10^{-8} cm s^{-1}	Total conductance from Fraser *et al.* (2011)
$P_{K(s)}$	Surface membrane background K^+ permeability	6.3×10^{-7} cm s^{-1}	
$P_{Cl(s)}$	Surface membrane background Cl^- permeability	2.7×10^{-6} cm s^{-1}	P_{Na}/P_K model-derived to give reasonable potentials; P_{Cl}/P_K ratio from Dulhunty (1979)
$P_{Na(t)}$	Tubular membrane background Na^+ permeability	2.4×10^{-12} cm s^{-1}	Base case assumptions only; variations in these parameters were explored during the study
$P_{K(t)}$	Tubular membrane background K^+ permeability	$= P_{K(s)}$	
$P_{Cl(t)}$	Tubular membrane background Cl^- permeability	$= P_{Cl(s)}$	
$[Na^+]_e$	Extracellular Na^+ concentration	147 mM	
$[K^+]_e$	Extracellular K^+ concentration	4 mM	
$[Cl^-]_e$	Extracellular Cl^- concentration	151 mM	
z_{Xt}	Valency of fixed osmolytes in the t-system	0, or range from $+\infty$ to $-\infty$ (mol^{-1})	

Extracellular ion concentrations, membrane permeabilities, pump densities and z_{Xt} were all varied in turn during this study to determine their effects on t-volume. Where not specified in the text, parameters took on values provided in this table. Note that membrane potentials, compartmental volumes and intracellular and intra-t-system ion concentrations are dependent variables with steady-state values that are uniquely determined by the parameter set listed in this table.

t-system cannot be treated as a rigid structure. Yet, a model t-system not subject to relative hydrostatic pressures, and containing no fixed osmotic or charged contents relative to other compartments, is unconstrained (Rapoport, 1969), with no single steady-state volume. Any process driving ions into or out of the t-system on net would then produce indefinite swelling or shrinkage. However, experimental evidence shows that the t-system has a limited capacity to shrink (Launikonis & Stephenson, 2002), suggestive of the influence of negative hydrostatic pressure at low t-volumes. In contrast, the t-system is able to swell enormously (Krolenko & Lucy, 2001) suggesting little influence of positive hydrostatic pressure at larger volumes. Finally, the t-system may also contain fixed charges and/or osmoles (Rapoport, 1969). These properties are not mutually exclusive – for instance, proteoglycans in the t-system could physically resist t-system shrinkage (Davis & Carlson, 1995) while contributing a small charge and osmotic effects.

We therefore sought to model the effects of positive and negative hydrostatic pressures, fixed osmolytes and fixed charges in the t-system. The effects of negative hydrostatic pressure and osmotic pressure are mathematically similar and both vary in proportion to compartment volume. Thus, negative hydrostatic pressures were not explicitly simulated in the analysis. Instead, the effects of negative pressures and fixed osmolytes were jointly simulated using a single pair of terms representing osmotic content and charge fixed in the t-system, impermeant to all other compartments.

Constraints of fixed charge and osmolality in the transverse tubular system

Fixed solutes (X_t) in the t-system were simulated, as for other ions, as a concentration $[X]_t$ (mosmol l^{-1}), and is thus a dependent variable of the model with a unique steady-state value defined by the parameter set. In contrast, the charge valency of X_t (z_t; mosmol^{-1}) is a parameter of the model. This gave three limiting cases that were explored in detail: fixed osmotic activity with no fixed charge, and fixed positive or negative charges with no fixed osmotic activity. Note that in the two limiting cases of no fixed osmotic activity (or, equivalently, no negative pressure) in the t-system (denoted as $z_t = +\infty$ or $z_t = -\infty$), $[X]_t$ instead represented a charge concentration per litre. This too is a dependent variable of the model, though the sign of its charge (+ or –) is a parameter.

A history-independent model of transverse tubular volume

To define a relationship between model parameters and steady-state values of the modelled variables, such as intracellular concentrations and E_m, each parameter set must give a unique set of solutions for all variables. Figure 2 demonstrates that steady-state ion concentrations and membrane potentials in all modelled compartments are indeed independent of the intracellular or t-system ion concentrations used at the start of each simulation.

Results

We sought to define the minimum conditions for stabilizing a t-system containing fixed charge (z_t) and/or fixed osmotic content (X_t). As solutes in the ECF can enter the t-system, the presence of X_t or z_t forms a 'single Donnan' system (Fraser & Huang, 2004) across the access resistance that drives net ion and water fluxes from the ECF into the t-system. This precludes *passive* t-volume stability without positive hydrostatic pressures, as earlier suggested by Rapoport (1969). However, the presence of Na^+ leak currents and active Na^+/K^+ transport precludes accurate treatment of the t-system as a passive double Donnan system. Furthermore, it cannot explain t-volume changes with, for example, Na^+/K^+-ATPase inhibition, or transient changes in t-volume. Instead, our simulations demonstrate that t-volume stability can be maintained by active ion transport in the absence of any stabilizing hydrostatic pressure. This suggests an alternative *active* model of t-volume determination and regulation.

In this model, net ion uptake from the ECF into the t-system is offset by a second net flux of ions from the t-system into the sarcoplasm, ultimately balanced by a third net flux to the ECF across the sarcolemma. The active transport of Na^+ and K^+ across the sarcolemma and tubular membrane permits ions to be kept out of equilibrium across the access resistance. Yet for t-volume to be stable, the net flux of ions shifting from compartment to compartment must be equal, forming a net ion cycle powered by the Na^+/K^+-ATPase at rest.

Figure 3 demonstrates the parameter sets that produce a large enough net ion flux from the t-system→sarcoplasm

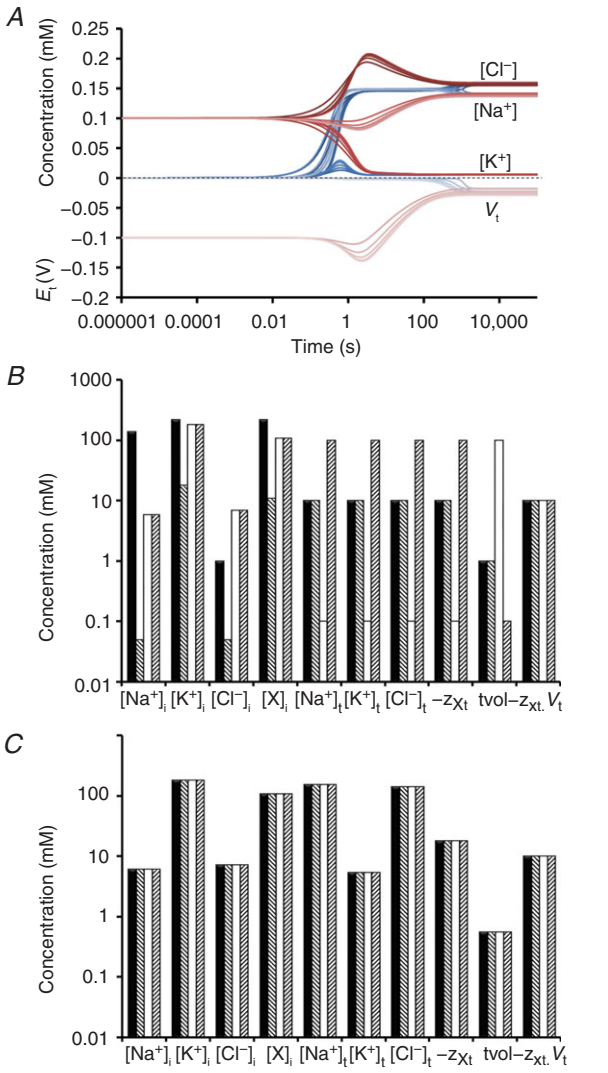

Figure 2. A history-independent model of muscle fibre electrophysiology and t-system volume
To investigate factors determining ion concentrations, membrane potentials and volumes of the sarcoplasm and t-system at rest, their steady-state values must be independent of their historical values. The present muscle fibre model demonstrates this property. *A*, when the model is initialized with two arbitrary sets of concentration variables (red and blue lines respectively, every fourth t-system shell depicted in each case), these variables relax over time to attain identical steady-state values. These are independent of their values at $t = 0$ ('history independent') and therefore determined only by the model parameters listed in Table 1. The model demonstrates history independence even when a wider range of initial values is used – compare (*B*), showing values of modelled variables at $t = 0$ to (*C*), showing steady-state values at $t = \infty$.

to offset the net ECF→t-system fluxes produced by the presence of X_t or z_t in the absence of any physical constraints on t-volume. Simulations were performed to study the influence on t-volume of distributions of P_{Na}, P_K and Na^+/K^+-ATPase density between the t-system and surface membrane. Distributions ranging from 100% in the t-system to 100% in the sarcolemma were explored for all combinations in five equal steps for each. The stability maps were similar across all the limiting values of z_t and X_t, so only one example, where z_t is negative and $X_t = 0$, is shown.

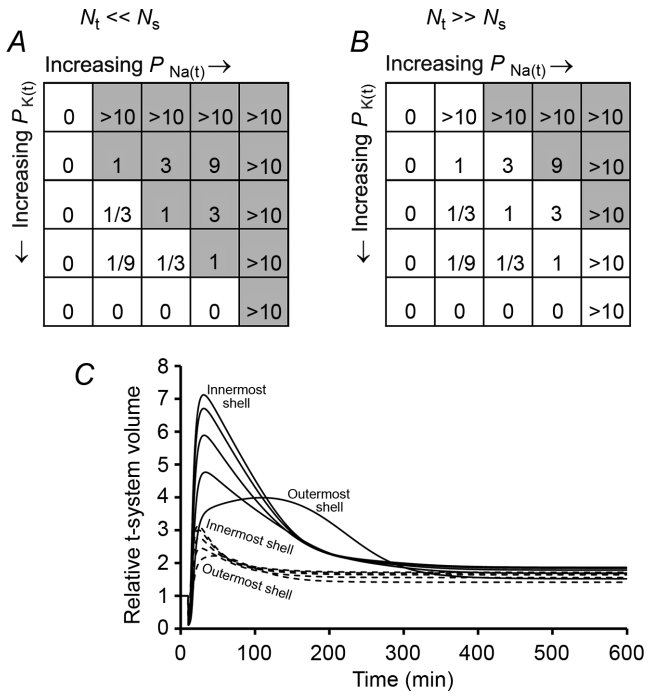

Figure 3. T-system volume is constrained and stabilized by active ion pumping and ion leakage
The stability of the modelled t-system volume depends on the distribution of Na^+ and K^+ channels and the Na^+/K^+-ATPase between the t-system and the sarcolemma. The numbers in this figure denote the ratio $P_{Na(t)}/P_{K(t)}$ expressed relative to the ratio $P_{Na(s)}/P_{K(s)}$ [i.e. $(P_{Na(t)}/P_{K(t)})/(P_{Na(s)}/P_{K(s)}$]. Shading denotes the sets of ion permeabilities that produce stable t-system volumes; unshaded boxes denote parameter sets that produce continual swelling in the absence of opposing pressure. The influence of the Na^+/K^+-ATPase distribution (N_t/N_s) on t-system stability can be seen by comparing (*A*) (low N_t/N_s) with (*B*) (high N_t/N_s). T-system stability requires $P_{Na(t)}/P_{K(t)} \geq P_{Na(s)}/P_{K(s)}$ if N_t/N_s is low, and $P_{Na(t)}/P_{K(t)} >> P_{Na(s)}/P_{K(s)}$ if N_t/N_s is high. Thus, channel distributions that polarize the sarcolemma relative to the t-system favour t-volume stability. *C*, demonstrates the effects of acute alterations to Na^+/K^+-ATPase activity, revealing transient as well as steady-state t-volume changes. A t-system at steady state was subject to ATP depletion (to 1/10th of resting levels), ADP accumulation (250-fold increase) and P_i accumulation (10-fold increase) to an extent seen in intense exercise (solid lines) (Dawson *et al.* 1980; Nagesser *et al.* 1993), or to half that extent (dashed lines). The resultant impaired Na^+/K^+-ATPase activity led to triphasic changes: transient shrinkage of the t-system as loss of electrogenic polarization allows a Cl^- influx into the cell; then t-system swelling over hours as ion fluxes re-equilibrate, before a gradual and incomplete recovery to a swollen steady-state t-volume. The transient volume changes were greater and more prolonged in the outer regions of the t-system.

For a stable t-volume in the presence of z_t, X_t, or negative hydrostatic pressure, the P_{Na}/P_K ratio needs to be greater for the t-system membrane than for the sarcolemma, and even more so if the Na^+/K^+-ATPase density is greater in the t-system membrane than the sarcolemma. The model predicts that for any set of 'stable' t-system parameters, when the cell is energetically compromised, transient and baseline changes in t-volume result (Fig. 3). These underscore the importance of the Na^+/K^+-ATPase in maintaining not just t-system stability, but also its absolute volume over time. In contrast, the distribution of Cl^- permeability was found not to influence t-volume. This is expected, as the net Cl^- flux must be zero across all resistances at steady state, unless it is actively transported.

We therefore show that t-volume stability is possible even in the absence of hydrostatic pressure gradients, although we do not and cannot exclude their presence. Instead, we note that physical constraints might be expected to produce pressures that oppose volume changes, but would not be expected to influence whether a particular experimental manoeuvre produced swelling or shrinkage.

Figure 4 illustrates the ion fluxes observed in steady-state t-systems having the 'stabilizing' properties proposed in Fig. 3 of $(P_{Na(t)}/P_{Na(s)}) > (P_{K(t)}/P_{K(s)})$ and/or $N_t < N_s$. Na^+ and K^+ ions cycle in opposite directions, with the flux of Na^+ being larger. The net circuit flux at rest is therefore equal to the magnitude of the Na^+ flux minus the magnitude of the K^+ flux.

Figure 5A relates ion cycles to cell volume. For all the parameter sets shown to produce a stable t-volume in Fig. 3 and others, the t-volume was plotted against the magnitude of the net ECF → t-system → sarcoplasm → ECF ('circuit') ion cycle at rest. For comparison, t-volumes are normalized to their value at a flux of 100 μmol l^{-1} s^{-1}. There is a clear and consistent relationship between t-volume and the magnitude of circuit flux. Larger circuit fluxes produce a smaller t-system. A potential difference accompanies any circuit flux through the access resistance, equivalent to the difference between surface and tubular membrane potentials. This potential is influenced by fixed charge in the t-system. For any given fixed charge, the magnitude of the potential and the magnitude of circuit flux are almost directly proportional (Fig. 5B).

Comparisons with previous experimental data

The account of t-volume suggested by Figs 3–5 is testable against known experimental outcomes. The remainder of this work tests model predictions against previous

experimental findings from all studies concerning t-system behaviour with different ECF osmolalities and solute composition. To do this, it was necessary to select a baseline parameter set. Assumptions were made that permitted a stable model t-system and also agreed with previous experimental findings: thus $N_t < N_s$ (Narahara *et al.* 1979; Venosa & Horowicz, 1981), $P_{Na(t)} > P_{Na(s)}$ (Fig. 3), $P_{K(t)} = P_{K(s)}$ (Dulhunty, 1979) and negative z_t were chosen (Davis & Carlson, 1995). $P_{Cl(t)} = P_{Cl(s)}$ was assumed for the base case, though the consequences of this assumption were explored as the distribution of Cl^- conductances in skeletal muscle is controversial (Dulhunty, 1979; Dutka *et al.* 2008; Lueck *et al.* 2010; DiFranco *et al.* 2011; Lamb *et al.* 2011). A t-system model with the chosen baseline parameters was simulated until all variables attained steady state. Then, simulations were conducted to replicate experimental protocols. The transient and steady-state t-volume changes observed were then compared with the experimental data.

The values of key physical parameters in various species that might allow prediction of absolute t-volumes according to our model are not known. However, as shown in Fig. 4, independent of the initial parameter set, circuit flux is still predictive of t-volume. Thus, while the chosen parameter set may not represent actual permeability or Na^+/K^+-ATPase distributions in any species, its behaviour is expected to be qualitatively similar to any parameter set that produces a stable t-volume. Furthermore, as discussed earlier, physical constraints on t-volume might change the magnitude but not the direction of t-volume changes relative to the predictions of the model.

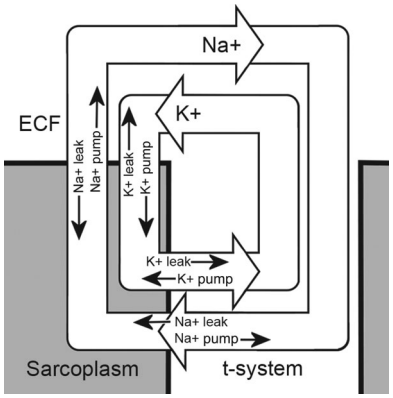

Figure 4. Net ion fluxes occur between the extracellular space, t-system and sarcoplasm even at steady state
In all t-systems that the model predicts to have stable volumes, at steady state, there is a net ion flux moving in a circuit from the extracellular space to the t-system, to the sarcoplasm, before returning once more to the extracellular space. Functionally, a net ion flux in this direction would deal with the t-system's tendency to swell from the direction of the ECF, as Donnan constraints predict. Mechanistically, this net flux arises from a small difference between the magnitudes of a net Na^+ flux, and a slightly smaller K^+ flux in the opposite direction. The net transmembrane Na^+ and K^+ fluxes themselves arise from small imbalances between the pump and leak fluxes in each membrane; thus, $J_{Na(leak)} > J_{Na(pump)}$ and $J_{K(leak)} > J_{K(pump)}$ across the t-system membrane, whereas $J_{Na(leak)} < J_{Na(pump)}$ and $J_{K(leak)} < J_{K(pump)}$ across the surface membrane. Factors that increase the net circuit flux magnitude reduce steady-state t-volume, while conversely, factors that decrease the net circuit flux magnitude result in t-system swelling. ECF, extracellular fluid.

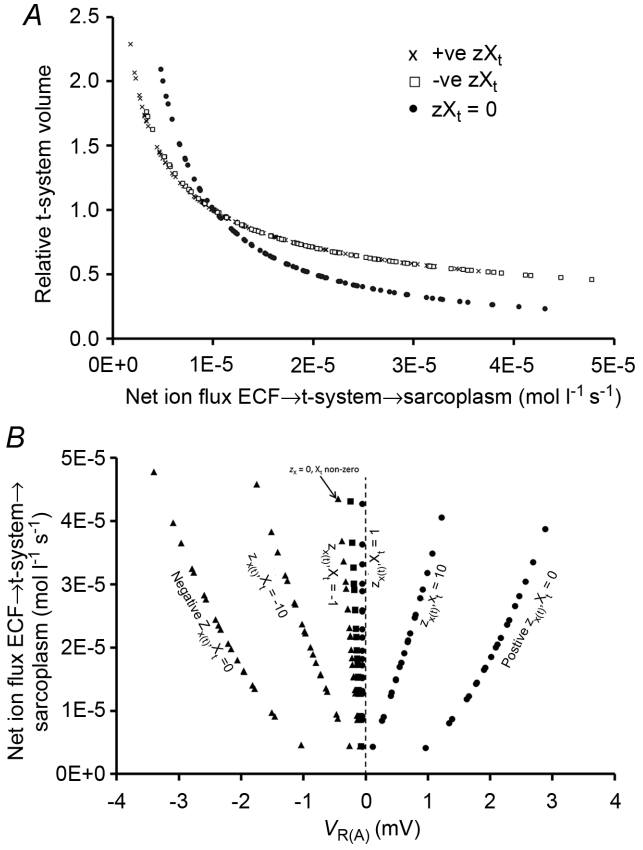

Figure 5. At rest, t-system volume is determined by the magnitude of the net ion flux circulating between the extracellular space, t-system and sarcoplasm
T-systems with different distributions of P_{Na}, P_K, P_{Cl} and N between the t-system and surface membranes were simulated. All combinations of $P_{Na(t)}/P_{Na(s)}$, $P_{K(t)}/P_{K(s)}$ and N_t/N_s distributions were simulated, each varied from 0 to 100% in five equally spaced values. For those parameter sets that produced a stable steady-state t-volume, the resultant steady-state net circuit fluxes and t-volumes are plotted in (*A*). At steady state, the magnitude of the net circuit flux moving ECF → t-system → sarcoplasm → ECF is inversely related to t-volume, regardless of the identities of ions or component fluxes contributing to it. The direction of the relationship between t-volume and circuit flux is preserved regardless of the nature of impermeants in the t-system (limiting cases where $z_t = -\infty$, $+\infty$ or 0 are shown – see Methods for the definition of this parameter). *B*, the nature of impermeants in the t-system influences the potential difference across the tubular access resistance. A more polarized t-system generates a larger circuit flux passing through the access resistance, and thus a smaller t-system volume. ECF, extracellular fluid.

Isotonic variation in $[NaCl]_e$

Since the 1960s, t-volume has been shown to change with extracellular ionic composition. Both Foulks *et al.* (1965) and Rapoport (1969) reported t-system diameter increases of >200% when extracellular NaCl was replaced with an equal osmolality of sucrose. This provided one of the first indications that t-volume was not solely determined by physical constraints or extracellular osmolality. These experiments were replicated with simulations, where extracellular NaCl was abruptly replaced with a membrane-impermeant solute of equivalent osmolarity, in a model fibre initially at steady state.

A simulated isotonic reduction in $[NaCl]_e$ produced marked t-system swelling (Fig. 6*A*), rapidly reaching a maximum volume within 5–20 min. T-volumes then partially recovered to a new steady state over 30–300 min. The swelling phase was faster and the partial recovery phase was slower with greater reductions in $[NaCl]_e$. The experiments of Rapoport (1969) recorded volumes after long (4 h) immersions in reduced $[NaCl]_e$ Ringer solutions, and thus Fig. 6*B* compares steady-state t-volumes from the model with Rapoport's experimental measurements of the t-system's longitudinally oriented diameter. Rapoport (1969) noted that the transversely oriented t-system diameter did not change with $[NaCl]_e$, and thus the t-volume might be expected to relate linearly to its longitudinally oriented diameter. Indeed, the t-volumes predicted by the model are in close agreement with the experimental diameter measurements.

The mechanism of the change in steady-state volume seen in the model may be straightforwardly explained in terms of ion cycling: t-volume increases because of a decrease in Na^+ cycling (see Figs 4 and 5) under conditions of reduced $[Na^+]_e$. The initial transient larger increase in volume is driven by Cl^- efflux, as described in more detail below (see Fig. 10).

Variations in extracellular osmolality at constant ionic strength

Another experimental manipulation that has received considerable attention is the increase in extracellular osmolality at constant ionic strength by the addition of sucrose to the extracellular medium (Dydynska *et al.* 1963; Freygang, 1964; Freygang *et al.* 1967; Franzini-Armstrong *et al.* 1978; Launikonis & Stephenson, 2002; Martin *et al.* 2003). In all cases, significant increases in t-system diameter or cross-sectional area were noted on exposure to hypertonic solutions (Freygang, 1964; Franzini-Armstrong *et al.* 1978; Martin *et al.* 2003). Where quantified, diameter or area increases of 2–4-fold were noted (Freygang, 1964; Launikonis & Stephenson, 2002; Martin *et al.* 2003), although other studies simply reported the existence of dilated vesicles within the fibres (Dydynska *et al.* 1963) or 'marked t-system swelling and vacuolation' (Franzini-Armstrong *et al.* 1978). Increases in t-system diameter from 9 min following exposure to sucrose (Franzini-Armstrong *et al.* 1978) have been noted to persist for more than an hour (Dydynska *et al.* 1963; Launikonis & Stephenson, 2002), but were not detected after 24 h exposures (Dydynska *et al.* 1963), strongly suggesting that certain t-volume changes are transient.

As shown in Fig. 7, the model also demonstrated marked and rapid increases in t-volume with the addition of a

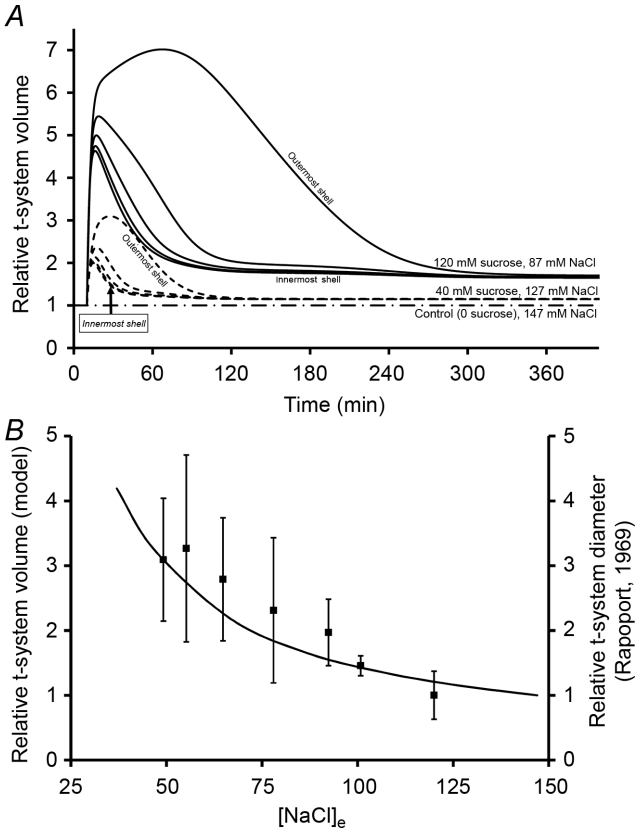

Figure 6. Isotonic reduction in $[NaCl]_e$ produces rapid t-system swelling followed by a partial recovery
The effect on t-system volume of isotonic replacement of NaCl with sucrose in simulations and previous experimental work is compared. *A*, simulations of the time course of mean volume changes in 20 t-system shells in response to the replacement of 20 mM or 60 mM NaCl with an osmotically equivalent sucrose concentration at 10 min. Five evenly spaced t-system shells are depicted in each case, including the outermost and innermost shells. Rapid t-system swelling is followed by a slower and only partial recovery to a swollen steady-state volume. Outer regions showed transient swelling that was up to 50% greater than the inner regions, then recovered more slowly yet reached almost identical steady-state volumes. *B*, compares the simulated steady-state inner t-system volumes for a range of $[NaCl]_e$ (solid line – simulations conducted at 10 mM increments from 37 to 147 mM $[NaCl]_e$) with comparable experiments in which t-system diameter was measured 4 h after exposure to test solutions (filled squares, mean ± SD, plotted from data in table II of Rapoport *et al.* 1969).

membrane-impermeant solute to the extracellular space. T-volumes remained swollen, particularly in the outer regions, for a prolonged period before finally returning to normal volumes after approximately 8 h, with such recovery occurring in the inner regions long before the outer regions. These findings of rapid t-system swelling, maintained over at least 1–2 h but resolving over much longer periods, agrees qualitatively with the experimental studies noted above. However, the degree of swelling in the model appears to exceed that reported elsewhere, except perhaps in the study of Franzini-Armstrong (1978). However, direct comparison of the model findings with earlier experimental results is problematic because simulated t-volume changes evolve over a prolonged period, and are significantly different in the inner and outer t-system. In contrast, available experimental studies have considered single time points and do not generally state the depth of the t-system being examined. It is also probable that the simulations overestimate the initial swelling phase, as the model does not simulate an increase in hydrostatic pressure, which might be expected to accompany and oppose such gross swelling. It is also possible that the increased Na^+-K^+-$2Cl^-$ cotransporter activity reported in hypertonic solutions and abolished by detubulation (Chin *et al.* 2004; Ferenczi *et al.* 2004; Fraser *et al.* 2006) may contribute to t-volume changes in hypertonic solutions.

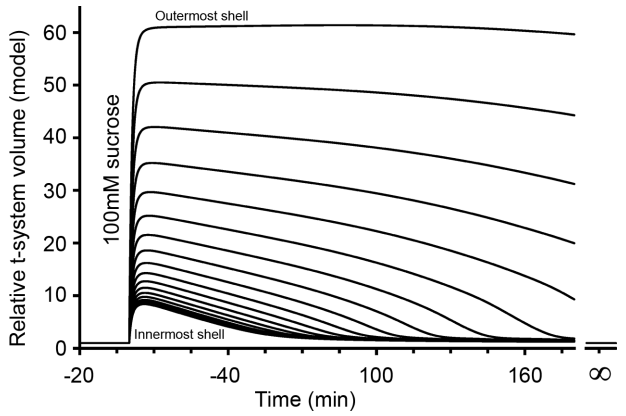

Figure 7. Sucrose addition causes temporary but prolonged t-system swelling
The volume of each of 20 t-system shells from the innermost (lowest trace) to the outermost (upper trace) is depicted following the addition of 100 mM sucrose to the extracellular space at time zero. Rapid and marked swelling occurs in all t-system shells, but is approximately 10-fold greater in the outermost than the innermost regions of the t-system. The t-system volume then recovers very slowly to almost precisely its normal steady-state value (~4% shrinkage, shown at $t = \infty$) despite the continued presence of sucrose in the extracellular space. Recovery is much faster in the inner segments than the outer, with the latter taking up to 8 h to return to normal volume.

The fast initial swelling arises in the model from sucrose diffusing into the t-system via the access resistance faster than water diffuses out of the sarcoplasm via the sarcolemma. An osmotic gradient then develops favouring water efflux from the sarcoplasm across the tubular membrane as well as the sarcoplasm. This causes rapid and marked t-system swelling, but because sucrose enters via the access resistance, the sucrose concentration rises earliest in the outer regions of the t-system, while water efflux into the t-system dilutes the sucrose concentration in the inner regions of the t-system. Thus, swelling is markedly greater in the outer regions of the t-system. All compartments become isotonic within 5 min, and the t-volume recovers thereafter as the relatively small circuit fluxes reassert themselves as the primary determinants of steady-state t-volume. However, t-volume recovery is slow relative to the initial swelling, and is much slower in the outer regions of the t-system, taking several hours in the simulation.

Anisotonic variation in extracellular NaCl

Several studies have explored how anisotonic variations in $[NaCl]_e$ affect t-volume, but with apparently contradictory results. Thus exposure to hypertonic high $[NaCl]_e$ solutions produced t-system swelling after 15–30 min in frog and after 10–60 min in rat (Davey & O'Brien, 1978; Franzini-Armstrong *et al.* 1978) but no significant change in t-volume after exposures of 'at least 30 min' in frog (Freygang *et al.* 1967). However, exposure to hypotonic 80 mM $[NaCl]_e$ solutions has also been shown to produce t-system swelling after 30 min in frog (Martin *et al.* 2003).

Figure 8 demonstrates simulations of changes in $[NaCl]_e$ to between 50 and 270 mM without any osmotic compensation. Exposure to anisotonic varied $[NaCl]_e$ solutions might be considered as a combination of the stresses imposed in Figs 6 and 7, or their effective opposites. Indeed, Fig. 8 shows that this produced the rapid (within <5 min) t-system swelling, as with the increased ECF osmolality depicted in Fig. 7. This was followed by slower shrinkage (over 1–2 h) to a shrunken steady state. Exposure to hypotonic low $[NaCl]_e$ solutions produced opposite volume changes, with rapid t-system shrinkage followed by swelling to reach a swollen steady state; the latter observation replicates the swelling with isotonic decreases in $[NaCl]_e$ depicted in Fig. 6. As in Fig. 6, these steady-state volume changes, reflect reduced net circuit flux in low $[NaCl]_e$ and increased net circuit flux in high $[NaCl]_e$ solutions.

The biphasic nature of these volume changes go some way towards reconciling contradictions between previous experimental findings. Thus, the finding of t-system swelling followed by slower shrinkage in hypertonic solutions may explain why t-system swelling was observed

by Davey and O'Brien (1978) and Franzini-Armstrong (1978), but not by Freygang *et al.* (1967). Similarly, the model predicts t-system swelling in hypotonic solutions developing from approximately 30 min, as observed by Martin *et al.* (2003).

Isotonic change of the $[K^+]_e/[Na^+]_e$ ratio

Isotonic replacement of extracellular Na^+ with K^+ has previously been shown to influence t-volume (Freygang, 1964; Usher-Smith *et al.* 2006*b*). Figure 9 shows the response of t-volume in muscles exposed to solutions of different $[K^+]_e$, while maintaining a constant value for the sum $[Na^+]_e + [K^+]_e$, and compares these to simulations. In each case, results are shown both in the presence of Cl^-, and in muscles equilibrated with Cl^--free solutions. Simulations in Cl^--free solutions (Fig. 9, solid line) show that increases in $[K^+]_e$ from the normal value of 2.5 mM produce a monophasic t-system swelling, reaching a new steady state relatively rapidly (between 30 and 100 min for 10 and 100 mM $[K^+]_e$ respectively). This increase in steady-state volume results from decreased Na^+ cycling, only partially offset by a slightly smaller decrease in K^+ cycling. Experimental measurements show similar increases in t-system diameter after 1 h (Fig. 9, filled triangles) (Usher-Smith *et al.* 2007). Reductions in $[K^+]_e$ below 2.5 mM also produce t-system swelling, in this latter case due to partial inhibition of the Na^+/K^+-ATPase activity and hence partial failure of ion cycling. However, there are no available experimental data below 2.5 mM $[K^+]_e$ in Cl^--free solutions.

Simulations of increased $[K^+]_e$ in Cl^--containing solutions show a more complicated picture due to cellular swelling, as has been reported in experiments (Usher-Smith *et al.* 2006*b*). This net cellular influx of K^+ and Cl^- drives water fluxes from the t-system as well as the ECF, transiently offsetting the tendency to swell seen in high $[K^+]_e$ Cl^--free solutions. T-volume thus takes longer to reach a steady state than in Cl^--free solutions. Simulation results are shown at 1 h (Fig. 9, long dashes) and 3 h (Fig. 9, short dashes) for comparison with experimental measurement at 1 h (Fig. 9, filled squares) (Usher-Smith *et al.* 2007). At 1 h in both simulations and experiments, the t-system is rather less swollen in high $[K^+]_e$ Cl^--containing solutions than in their Cl^--free equivalents.

Complete replacement of $[K^+]_e$ with $[Na^+]_e$ in Cl^--containing solutions causes an initial swelling phase similar to that seen in Cl^--free solutions as t-system ion cycling ceases due to the inhibition of Na^+/K^+-ATPase. However, although the initial effect of a zero $[K^+]_e$ solution is hyperpolarization, a slower depolarization then

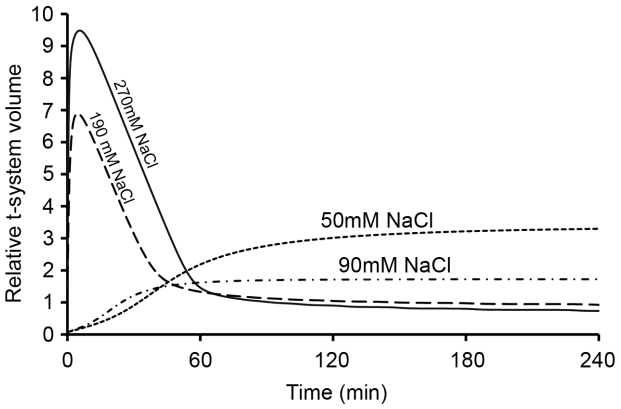

Figure 8. Anisotonic manipulation of extracellular [NaCl] leads to biphasic t-system volume changes
The mean t-system volume is shown for exposures at time zero of model fibres to solutions of reduced or increased [NaCl] without any osmotic compensation. Hypertonic high [NaCl] solutions produce a rapid and transient swelling that is followed by a slower shrinking phase that eventually produces a shrunken t-system at steady state. As with hypertonic sucrose addition (Fig. 7), hypertonic [NaCl] caused outer shells of the t-system to swell up to 10× more than the inner shells, and to recover more slowly, though eventual steady-state volumes were almost identical. Conversely, hypotonic low [NaCl] solutions produce rapid t-system shrinkage followed by a slower swelling phase, producing a swollen t-system at steady state. This initial shrinkage was up to 50% greater and recovered more slowly in the outer segments.

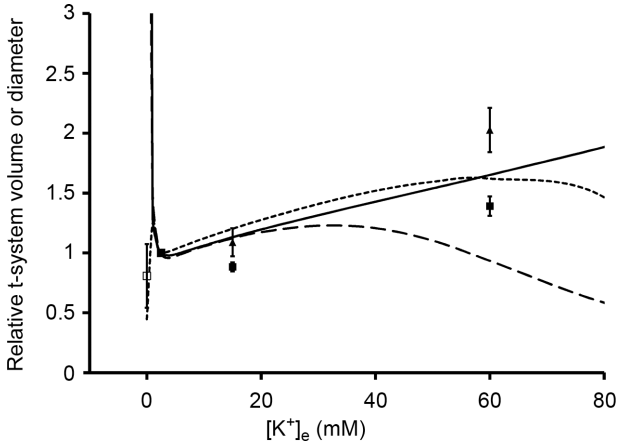

Figure 9. Isotonic replacement of Na^+ with K^+ influences t-system volume
Simulations are plotted as continuous lines for comparison with experimental results in Cl^--free (triangles) and Cl^--containing (squares) solutions. The solid symbols depict data from Usher-Smith *et al.* (2006*b*) after 1 h exposures to experimental solutions. The open symbols are data from Freygang *et al.* (1964) after an exposure of unknown duration. The solid line depicts simulations in Cl^--free solutions at steady state, which was reached in under 1 h. The broken lines show simulations of the t-system volume in Cl^--containing solutions at 1 h (long dashes) and at 3 h (short dashes). In each case, simulations were conducted for $[K^+]_e$ values between 0 and 80 mM, at 1 mM intervals to 10 mM and at 5 mM intervals thereafter. Volume changes were similar in all t-system shells (<10% variation between innermost and outermost shells).

develops and gradual NaCl influx pulls water from the ECF and the t-system, shrinking the t-system. This is perhaps the effect seen experimentally with complete K^+ withdrawal (Fig. 9, open square) (Freygang et al. 1964), although it is not clear how soon after K^+ withdrawal this measurement was made.

Isotonic withdrawal of extracellular Cl^-

Experimental studies have consistently noted t-system swelling on replacement of extracellular Cl^- with a membrane-impermeant ion (Freygang, 1964; Foulks *et al.* 1965; Dulhunty, 1982), though the conclusions drawn from this finding have differed. Thus, Foulks *et al.* (1965) and Dulhunty (1982) conclude that such swelling indicates Cl^- efflux across the t-system membranes and hence a high tubular Cl^- conductance. In contrast, Freygang *et al.* (1967) and Rapoport (1969) explain this finding as an effect of sucrose in the t-system or as being due to a decrease in the ionic strength of the solution.

Figure 10 compares these experimental results with simulations. Cl^- withdrawal, whether replaced with a monovalent (Fig. 10, solid line) or a divalent anion (Fig. 10, long dashes), produces transient t-system swelling, in broad agreement with the experimental results [Fig. 10, squares (monovalent) and circles (divalent)]. Simulations show both swelling and recovery that is faster than seen in the experiments of Dulhunty (1982) with the chosen parameter set. In further agreement with experimental results, complete inhibition of Cl^- channels prevents any t-volume changes on exposure to Cl^--free solutions (data not shown).

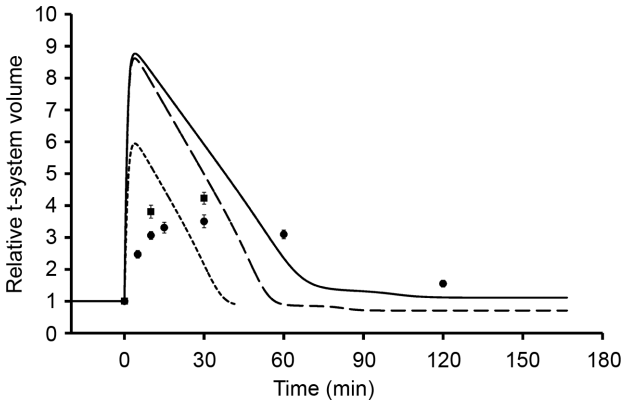

Figure 10. Isotonic Cl^- withdrawal causes transient t-system swelling
Simulations are compared with experimental data for the t-system volume during the replacement of NaCl with isotonic sodium methylsulphate (squares, experimental; solid line, simulation) or isotonic Na_2SO_4 (circles, experimental; long dashes, simulation). Experimental data are redrawn from Dulhunty (1982). In all cases, Cl^- withdrawal produces transient t-system swelling, which in the case of replacement with Na_2SO_4 is followed by steady-state t-system shrinkage. In addition, a simulation of Cl^- withdrawal for a model fibre with no t-system Cl^- permeability is shown (short dashes). In each case, the mean t-system volume is depicted: swelling was up to 50% greater and recovered more slowly in the outermost than the innermost t-system shells.

However, in contrast to previous assumptions, the location of Cl^- channels has only a marginal influence on how Cl^- withdrawal affects t-volume. In Fig. 10, the transient t-system swelling observed on Cl^- withdrawal is not abolished in simulations that locate all Cl^- channels on the surface membrane (Fig. 10, short dashes). The reason for this is that loss of Cl^- across the sarcolemma drives K^+ loss across both the sarcolemma and t-system membranes, rendering the cell slightly hypotonic relative to the ECF. This provokes water efflux, and because the t-system accounts for 80% of the total membrane area, the majority of the water efflux from the cell is via the t-system, even though the majority of the ion efflux occurs across the sarcolemma.

Addition and withdrawal of glycerol

Addition and withdrawal of a semi-membrane-permeant solute such as glycerol (Fraser *et al.* 1998; Krolenko & Lucy, 2001) or dimethyl sulphoxide (Fraser, 2011) causes pronounced vacuolation of the t-system. Importantly, this classic finding was reproduced in the present model. As depicted in Fig. 11, measurements have been made of amphibian skeletal muscle fibre volumes during the glycerol-induced vacuolation process, allowing calibration of the glycerol permeability term in the model. A glycerol permeability of 1×10^{-6} cm s^{-1} gives biphasic volume changes on addition and withdrawal of glycerol that adequately reproduce the experimentally recorded muscle fibre volume changes. The simulations predict rapid and gross t-system swelling on glycerol withdrawal that is greater than any other manipulation studied. Furthermore, they show that the innermost regions of the t-system swell sooner and more prominently than the outermost region, echoing experimental findings that vacuolation begins earliest in the fibre core (Fraser *et al.* 1998; Krolenko & Lucy, 2001). Finally, the swelling is very prolonged, eventually returning to steady-state values over as much as 20 h.

The model demonstrates that glycerol withdrawal from a glycerol-loaded fibre produces a brief initial t-volume decrease as the glycerol-loaded fibre takes up water from both the ECF and the t-system. Within 30 s, the t-system comes into osmotic equilibrium with the fibre, and thereafter glycerol and water efflux from the fibre into the ECF and the t-system causes fibre shrinkage and t-system swelling. Swelling is most prominent in areas furthest away from the surface, as glycerol efflux from the t-system across the access resistance is slowest from the deepest areas of the t-system.

Discussion

Regulation of the transverse tubular volume system is poorly understood

The volume and geometry of the t-system have been found to change with the composition of the ECF (Dydynska *et al.* 1963; Rapoport *et al.* 1969; Dulhunty, 1982; Launikonis & Stephenson, 2002, 2004; Fraser, 2011), in exercise, and in muscle disease (Gonzalez-Serratos *et al.* 1978; Casademont *et al.* 1988; Lännergren *et al.* 1990, 2000; Usher-Smith *et al.* 2007). Thus, a clear understanding of t-volume regulation is necessary to understand fully muscle fatigue, pathological changes and to inform experimental design. However, the mechanisms that determine t-volume at rest and following physiological and pathological stresses are poorly understood. A large number of experimental studies have attempted to address this question, leading to several competing theories of t-volume determination and regulation.

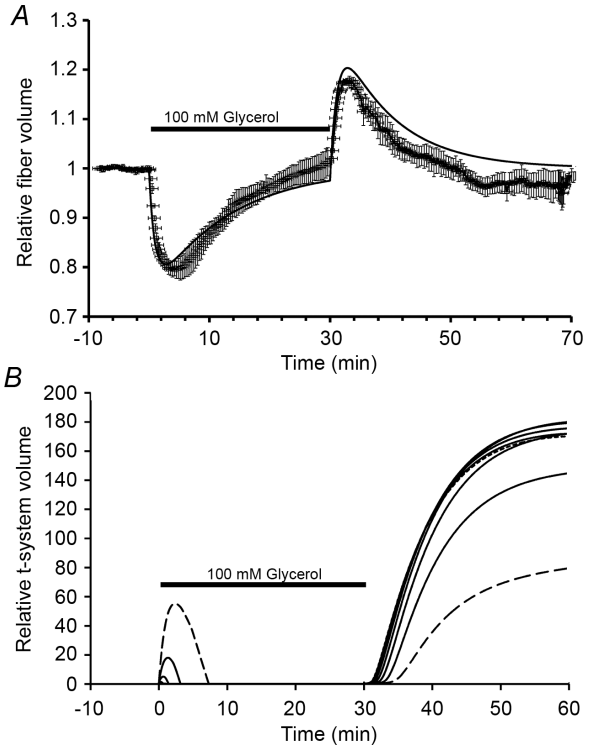

Figure 11. Glycerol addition induces transient t-system swelling; glycerol withdrawal induces vacuolation
Simulated and experimentally determined volumes during glycerol addition and withdrawal are compared here. *A*, fibre volumes are shown – filled squares (mean ± SD) are drawn from experimental data (Fraser *et al.* 1998), while simulation results are shown with a solid line, using a glycerol permeability term calibrated to reproduce these experimental data. *B*, simulated changes in the volume of every third t-system shell from the inner (short dashes) to outer (long dashes) shells. Transient t-system swelling occurs with glycerol addition, and the model recapitulates the profound t-volume increase seen experimentally as vacuolation on glycerol withdrawal, most prominently in the innermost parts of the t-system.

These previous accounts of t-volume regulation have been incomplete, and do not explain satisfactorily how t-volume changes with a full range of manipulations to ECF composition. Fatt (1964) proposed that the t-system contained impermeant charges relative to both the sarcoplasm and the ECF. With this in mind, Rapoport (1969) developed a Gibbs–Donnan equilibrium model of a t-system comprising negative charges stabilized by 'elastic constraint'. Freygang *et al.* (1967) and Rapoport *et al.* (1969) then surmised that the t-system swelled with decreasing ionic strength or increasing tonicity. However, this is not generalizable to cases where changing ionic composition alone changes t-volume, such as when Cl^- is replaced with methylsulphate. Similarly, explanations from a cell ↔ t-system flux theory (Dulhunty, 1982) cannot explain all observations consistently; for example, why biphasic volume changes are seen with NaCl addition or Cl^- withdrawal. The most recent account (Launikonis & Stephenson, 2002) surmised that t-volume shrank as E_m depolarized due to membrane-charge interactions, but this theory does not extend to explain the profound effects of uncharged solutes such as sucrose or glycerol.

The aim of the present study was therefore to produce a theory of t-volume determination and regulation that could provide a mechanistic, if qualitative, explanation of *all* available experimental studies. We employed a computer model of a skeletal muscle fibre and its t-system (Fraser *et al.* 2011) to investigate the determinants of t-volume at rest and to account for t-volume changes in response to altered ECF composition. The model was based on charge difference principles to ensure precise conservation of the relationships between charge, ion concentrations, osmolality and volume (Fraser & Huang, 2004, 2007). Predictions of the model were then compared with available experimental data.

Transverse tubular volume system homeostasis is an active process

We propose here a model of active t-volume homeostasis where a net circuit flux of ions exists at steady state, moving from the ECF → t-system → sarcoplasm → ECF. Our work culminates in the elegant finding that t-volume decreases as this circuit flux increases, and vice versa. We show that this circuit flux is sufficient to maintain t-volume stability, and is necessary to explain the direction of steady-state t-volume changes with the composition of the ECF. The circuit flux is ultimately dependent on Na^+/K^+-ATPase activity, but as pump activity tends to shrink the t-volume, it is probably opposed by factors that tend to swell the t-system. To this end, we also explored the effects of negative hydrostatic pressures, fixed

charges and/or mosmol in the t-system, showing that at least one such factor is needed to constrain t-volume to a single value. As these factors have mathematically similar effects on t-volume, it is not currently possible to employ our model to determine which of these physical factors has the greatest influence *in vivo*. Finally, the theory of active t-volume regulation presented here does not exclude the additional influence of structural elements and other physical factors, which are expected to constrain t-volume changes without influencing the direction of such changes.

A unifying account of transverse tubular volume

The primary novelty of our theory lies in its proposal that net fluxes across the surface and t-system membranes are different, yet in balance, at steady state. This produces a circuit flux, whose magnitude is the chief determinant of resting t-volume. The ECF composition determines the magnitude of component ion fluxes that sum to produce this net circuit flux, thus influencing t-volume in predictable ways. Our findings in this respect are summarized in Table 2. From the model, we conclude that manoeuvres reducing the circuit flux increase steady-state t-volume. The circuit flux consists of a Na^+ flux ECF → t-system → sarcoplasm → ECF, which is opposed by a slightly smaller K^+ flux in the opposite direction. T-system swelling will arise from changes that decrease the net Na^+ circuit flux, such as reduced net tubular membrane Na^+ influx, or reduced net sarcolemmal Na^+ efflux. Swelling will also result from manoeuvres that increase the net K^+ circuit flux, such as increased net tubular K^+ efflux or increased net sarcolemmal K^+ influx. This simplifies relationships between ECF solutes and t-volume, allowing them to be investigated in a more systematic manner.

Importantly, our model also distinguishes transient and steady-state t-volume changes in response to extracellular conditions. Ionic circuit fluxes that determine steady-state t-volume are small – approximately 10–20% the size of background Na^+ leak currents. This means, first, that t-volume relaxes to steady state very slowly following perturbations, with volume stability not achieved for as long as 10–20 h in simulations of glycerol manipulations, for instance, replicating experimental findings (Krolenko *et al.* 1995). Secondly, manoeuvres that produce relatively rapid alterations to t-volume may initially act with little opposition from the circuit fluxes that work to stabilize volume. Thus, t-volume changes are often biphasic, with a rapid, passive phase being followed by a much slower phase that depends ultimately on Na^+/K^+-ATPase activity. These findings have implications for experimental design, as published studies have rarely been designed to capture these biphasic volume changes.

A further prediction of the simulations that has been recognized in some earlier experimental work is that outer and inner regions of the t-system may behave differently during rapid t-system swelling, although much smaller regional differences are seen with slower volume changes. Thus, application of hypertonic solutions produces much greater swelling in the outer regions, whereas glycerol withdrawal produces greater swelling in the inner regions, perhaps accounting for the observed t-system vacuolation. However, it should be recognized that the model may overestimate swelling due to the assumption that hydrostatic pressure is zero, or underestimate it under conditions where the t-system access resistance might be reduced, as has been suggested may underlie glycerol-induced detubulation. Significant differences between species, and in particular between mammalian and amphibian experimental systems, would be expected to influence the magnitude of the observed changes. Furthermore, recent findings suggest a higher density of t-tubules in the subsarcolemmal region (Jayasinghe & Launikonis, 2013) that might provide a partial buffer to volume changes.

Implications for understanding the transverse tubular volume system in active muscle

Some of the findings may provide a partial explanation for the t-system swelling and vacuolation described after intensive muscle stimulation (Gonzalez-Serratos *et al.* 1978; Usher-Smith *et al.* 2007). The present work shows significant t-system swelling with energy depletion (Fig. 3), and more modest t-system swelling with raised extracellular $[K^+]$ (Fig. 9), both of which have previously been identified in fatigued muscle. By analogy with glycerol efflux (Fig. 11), it also seems probable that lactate efflux might further contribute to t-system swelling, as has been suggested by earlier experiments (Lännergren *et al.* 1990).

However, these changes induce t-system swelling over different timeframes, to different extents and through different mechanisms. To understand t-volume changes during and after exercise, a model that incorporates voltage-gated channels, rectification, metabolic changes, pH homeostasis, physical movement and structural factors would be helpful. However, some parameters crucial to such a study remain ill defined. For example, the distribution of voltage-gated channels between the surface and tubular membranes might be expected to influence significantly t-volume changes in active muscle.

A useful account of the transverse tubular volume system

This study provides a qualitative account of t-volume in resting muscle that adequately predicts the direction of volume changes, relative magnitudes and time

Table 2. A summary of t-system volume responses to experimental manipulations

Change in ECF composition/experimental manipulation	Transient change in t-volume	Steady-state change in t-volume
↑ ECF osmolality (Figs 7, 8, 11)	Swelling +++ Osmolyte ECF → t-system ∴ water flux sarcoplasm → t-system	Swelling + Cell shrinkage increases $[K^+]_i$ ∴ K^+ ion cycle increases ∴ net circuit flux reduces.
↓ $[Na^+]_e$ (Figs 6, 8)	No transient change	Swelling ++ Na^+ ion cycle reduces ∴ net circuit flux reduces.
↑ $[K^+]_e$ (Fig. 9)	No transient change	Swelling + K^+ ion cycle increases ∴ net circuit flux reduces
↓ $[Cl^-]_e$ (Fig. 10)	Swelling ++ Cl^- sarcoplasm → t-system ∴ K^+ and water sarcoplasm → t-system	No steady-state change (Cl− is passively distributed ∴ does not contribute to the circuit flux)
Partial Na^+/K^+-ATPase inhibition (Fig. 3)	Swelling ++ Net K^+, hence Cl− and water fluxes sarcoplasm → t-system	Swelling + Decreased net circuit flux

The proposed circuit flux model of t-volume homeostasis adequately explains both transient and steady-state t-volume changes arising from manipulations of extracellular fluid (ECF) composition. These are summarized here with brief notes on the underlying mechanism for the volume changes in each case – see Figs 4 and 5 for a description of the circuit flux model. Note that each row of the table summarizes a single experimental manipulation, with all other experimental parameters, such as osmolality, kept constant unless otherwise specified. The number of '+' symbols shows the approximate magnitude of each t-volume change relative to others depicted in this table, allowing the effect of combined experimental manipulations, such as the hypertonic addition of NaCl, to be surmised.

courses resulting from different manoeuvres in all available experimental results. It is not intended to predict the absolute magnitudes or time courses of such changes, which would require an improved quantitative characterization of the physical properties and the geometry of the t-system. Furthermore, available experiments were performed in a range of species, preparations and experimental solutions. Nevertheless, with an improved mechanistic understanding of t-volume changes – in particular, the recognition that such changes are often biphasic – novel experiments can be designed to quantify better the unknown parameters.

Finally, the model allows prediction of how t-volume could be affected by the location or size of other ion fluxes, pharmacological manipulations or the energy status of the muscle fibre. For instance, the relative abundance of the Na^+-K^+-$2Cl^-$ cotransporter on the surface compared to the tubular membrane (Kristensen *et al.*, 2006) might be expected to drive ions opposite to the circuit flux, swelling the t-system. The distribution of P_{Cl} between surface and tubular membranes has long been a point of contention (DiFranco *et al.*, 2011; Lueck *et al.* 2010), but we demonstrate here that it makes little difference to an active regulation of resting t-volume. The concept that resting t-volume is actively regulated by ion cycles, not specifically by ionic strength or tonicity, and over and above physical constraint, gives us a new basis for understanding t-system electrophysiology and homeostasis. It suggests yet another way skeletal muscle function and energy status are coupled, and points towards direct causal links between dynamic changes in ion fluxes, t-system structure and function in active muscle. These represent important steps in advancing our understanding of muscle fatigue and myopathies.

References

Atkinson JB, Swift LL & Lequire VS (1981). Myotonia congenita. A histochemical and ultrastructural study in the goat: comparison with abnormalities found in human myotonia dystrophica. *Am J Pathol* **102**, 324–335.

Casademont J, Carpenter S & Karpati G (1988). Vacuolation of muscle fibers near sarcolemmal breaks represents T-tubule dilatation secondary to enhanced sodium pump activity. *J Neuropathol Exp Neurol* **47**, 618–628.

Chin DXL, Fraser JA, Usher-Smith JA, Skepper JN & Huang CLH (2004). Detubulation abolishes membrane potential stabilization in amphibian skeletal muscle. *J Muscle Res Cell Motil* **25**, 379–387.

Davey DF & O'Brien GM (1978). The sarcoplasmic reticulum and T-system of rat extensor digitorum longus muscles exposed to hypertonic solutions. *Aust J Exp Biol Med Sci* **56**, 409–419.

Davis AK & Carlson SS (1995). Proteoglycans are present in the transverse tubule system of skeletal muscle. *Matrix Biol* **14**, 607–621.

Dawson MJ, Gadian DG & Wilkie DR (1980). Studies of the biochemistry of contracting and relaxing muscle by the use of 31P n.m.r. in conjunction with other techniques. *Philos Trans R Soc Lond B Biol Sci* **289**, 445–455.

DiFranco M, Herrera A & Vergara JL (2011). Chloride currents from the transverse tubular system in adult mammalian skeletal muscle fibers. *J Gen Physiol* **137**, 21–41.

Dulhunty A (1982). Effect of chloride withdrawal on the geometry of the T-tubules in amphibian and mammalian muscle. *J Membr Biol* **67**, 81–90.

Dulhunty AF (1979). Distribution of potassium and chloride permeability over the surface and T-tubule membranes of mammalian skeletal muscle. *J Membr Biol* **45**, 293–310.

Dutka TL, Murphy RM, Stephenson DG & Lamb GD (2008). Chloride conductance in the transverse tubular system of rat skeletal muscle fibres: importance in excitation-contraction coupling and fatigue. *J Physiol* **586**, 875–887.

Dydynska M, Wilkie D, Huxley H & Page S (1963). The osmotic properties of striated muscle fibres in hypertonic solutions. *J Physiol* **169**, 312–329.

Ferenczi EA, Fraser JA, Chawla S, Skepper JN, Schwiening CJ & Huang CL-H (2004). Membrane potential stabilization in amphibian skeletal muscle fibres in hypertonic solutions. *J Physiol* **555**, 423–438.

Foulks J, Pacey J & Perry FFA (1965). Contractures and swelling of the transverse tubules during chloride withdrawal in frog skeletal muscle. *J Physiol* **180**, 96–115.

Franzini-Armstrong C, Heuser JE, Reese TS, Somlyo AP & Somlyo A V (1978). T-tubule swelling in hypertonic solutions: a freeze substitution study. *J Physiol* **283**, 133–140.

Fraser JA (2011). Dimethyl sulphoxide addition or withdrawal causes biphasic volume changes and its withdrawal causes t-system vacuolation in skeletal muscle. *J Physiol* **589**, 5555–5556; author reply 5557.

Fraser JA & Huang CL-H (2004). A quantitative analysis of cell volume and resting potential determination and regulation in excitable cells. *J Physiol* **559**, 459–478.

Fraser JA & Huang CL-H (2007). Quantitative techniques for steady-state calculation and dynamic integrated modelling of membrane potential and intracellular ion concentrations. *Prog Biophys Mol Biol* **94**, 336–372.

Fraser JA, Skepper JN, Hockaday AR & Huang CL (1998). The tubular vacuolation process in amphibian skeletal muscle. *J Muscle Res Cell Motil* **19**, 613–629.

Fraser JA, Wong KY, Usher-Smith JA & Huang CL-H (2006). Membrane potentials in Rana temporaria muscle fibres in strongly hypertonic solutions. *J Muscle Res Cell Motil* **27**, 591–606.

Fraser JA, Huang CL-H & Pedersen TH (2011). Relationships between resting conductances, excitability, and t-system ionic homeostasis in skeletal muscle. *J Gen Physiol* **138**, 95–116.

Freygang WH (1964). The relation between the late after-potential and the size of the transverse tubular system of frog muscle. *J Gen Physiol* **48**, 235–263.

Freygang WH, Goldstein DA, Hellam DC & Peachey LD (1964). The relation between the late after-potential and the size of the transverse tubular system of frog muscle. *J Gen Physiol* **48**, 235–263.

Freygang WH, Rapoport SI & Peachey LD (1967). Some relations between changes in the linear electrical properties of striated muscle fibers and changes in ultrastructure. *J Gen Physiol* **50**, 2437–2458.

Frigeri A, Nicchia GP, Balena R, Nico B & Svelto M (2004). Aquaporins in skeletal muscle: reassessment of the functional role of aquaporin-4. *FASEB J* **18**, 905–907.

Gonzalez-Serratos H, Somlyo AV, McClellan G, Shuman H, Borrero LM & Somlyo AP (1978). Composition of vacuoles and sarcoplasmic reticulum in fatigued muscle: electron probe analysis. *Proc Natl Acad Sci U S A* **75**, 1329–1333.

Hallerdei J, Scheibe RJ, Parkkila S, Waheed A, Sly WS, Gros G, Wetzel P & Endeward V (2010). T tubules and surface membranes provide equally effective pathways of carbonic anhydrase-facilitated lactic acid transport in skeletal muscle. *PLoS One* **5**, e15137.

Hernandez J, Fischbarg J & Liebovitch LS (1989). Kinetic model of the effects of electrogenic enzymes on the membrane potential. *J Theor Biol* **137**, 113–125.

Jayasinghe ID & Launikonis BS (2013). Three-dimensional reconstruction and analysis of the tubular system of vertebrate skeletal muscle. *J Cell Sci* **126**, 4048–4058.

Krolenko SA, Amos WB & Lucy JA (1995). Reversible vacuolation of the transverse tubules of frog skeletal muscle: a confocal fluorescence microscopy study. *J Muscle Res Cell Motil* **16**, 401–411.

Krolenko SA & Lucy JA (2001). Reversible vacuolation of T-tubules in skeletal muscle: mechanisms and implications for cell biology. *Int Rev Cytol* **202**, 243–298.

Lamb GD, Murphy RM & Stephenson DG (2011). On the localization of ClC-1 in skeletal muscle fibers. *J Gen Physiol* **137**, 327–329; author reply 331–333.

Lännergren J, Westerblad H & Flock B (1990). Transient appearance of vacuoles in fatigued Xenopus muscle fibres. *Acta Physiol Scand* **140**, 437–445.

Lännergren J, Bruton JD & Westerblad H (2000). Vacuole formation in fatigued skeletal muscle fibres from frog and mouse: effects of extracellular lactate. *J Physiol* **526**(Pt 3), 597–611.

Launikonis BS & Stephenson DG (2002). Tubular system volume changes in twitch fibres from toad and rat skeletal muscle assessed by confocal microscopy. *J Physiol* **538**, 607–618.

Launikonis BS & Stephenson DG (2004). Osmotic properties of the sealed tubular system of toad and rat skeletal muscle. *J Gen Physiol* **123**, 231–247.

Lueck JD, Rossi AE, Thornton CA, Campbell KP & Dirksen RT (2010). Sarcolemmal-restricted localization of functional ClC-1 channels in mouse skeletal muscle. *J Gen Physiol* **136**, 597–613.

Martin CA, Petousi N, Chawla S, Hockaday AR, Burgess AJ, Fraser JA, Huang CLH & Skepper JN (2003). The effect of extracellular tonicity on the anatomy of triad complexes in amphibian skeletal muscle. *J Muscle Res Cell Motil* **24**, 407–415.

Maughan DW & Godt RE (2001). Protein osmotic pressure and the state of water in frog myoplasm. *Biophys J* **80**, 435–442.

Maughan D & Recchia C (1985). Diffusible sodium, potassium, magnesium, calcium and phosphorus in frog skeletal muscle. *J Physiol* **368**, 545–563.

Nagesser AS, Van der Laarse WJ & Elzinga G (1993). ATP formation and ATP hydrolysis during fatiguing, intermittent stimulation of different types of single muscle fibres from Xenopus laevis. *J Muscle Res Cell Motil* **14**, 608–618.

Narahara HT, Vogrin VG, Green JD, Kent RA & Gould MK (1979). Isolation of plasma membrane vesicles, derived from transverse tubules, by selective homogenization of subcellular fractions of frog skeletal muscle in isotonic media. *Biochim Biophys Acta* **552**, 247–261.

Rapoport SI (1969). A fixed charge model of the transverse tubular system of frog sartorius. *J Gen Physiol* **54**, 178–187.

Rapoport SI, Peachey LD & Goldstein DA (1969). Swelling of the transverse tubular system in frog sartorius. *J Gen Physiol* **54**, 166–177.

Tanaka K (1978). Self-diffusion coefficients of water in pure water and in aqueous solutions of several electrolytes with 18O and 2H as tracers. *J Chem Soc Faraday Trans 1* **74**, 1879–1881.

Thompson L V & Fitts RH (1992). Muscle fatigue in the frog semitendinosus: role of the high-energy phosphates and Pi. *Am J PhysiolCell Physiol* **263**, C803–C809.

Usher-Smith JA, Skepper JN, Fraser JA & Huang CL-H (2006). Effect of repetitive stimulation on cell volume and its relationship to membrane potential in amphibian skeletal muscle. *Pflugers Arch* **452**, 231–239.

Usher-Smith JA, Fraser JA, Huang CL-H & Skepper JN (2007). Alterations in triad ultrastructure following repetitive stimulation and intracellular changes associated with exercise in amphibian skeletal muscle. *J Muscle Res Cell Motil* **28**, 19–28.

Venosa R & Horowicz P (1981). Density and apparent location of the sodium pump in frog sartorius muscle. *J Membr Biol* **59**, 225–232.

Wallinga W, Meijer SL, Alberink MJ, Vliek M, Wienk ED & Ypey DL (1999). Modelling action potentials and membrane currents of mammalian skeletal muscle fibres in coherence with potassium concentration changes in the T-tubular system. *Eur Biophys J* **28**, 317–329.

Wolosin JM & Ginsburg H (1975). The permeation of organic acids through lecithin bilayers. Resemblance to diffusion in polymers. *Biochim Biophys Acta* **389**, 20–33.

Woodbury JW & Miles PR (1973). Anion conductance of frog muscle membranes: one channel, two kinds of pH dependence. *J Gen Physiol* **62**, 324–353.

Additional information

Competing interests

None

Author contributions

J.A.F. developed the computer model used in this work and conceived the study. J.A.F. and J.S. jointly designed and performed the simulation experiments, analysed and interpreted the data, and drafted and revised the article.

Funding

J.A.F. was supported by a David Phillips Fellowship (BB/FO23863/1) awarded by the Biotechnology and Biological Sciences Research Council (UK). J.S. was supported by the Agency for Science, Technology and Research (Singapore) and a Caius Medical Association summer studentship from Gonville and Caius College, University of Cambridge.

Acknowledgments

We are grateful to Prof. C.L.-H. Huang for helpful discussions.